Received 27 August 2020; revised 23 November 2020; accepted 29 November 2020. Date of publication 3 December 2020; date of current version 28 January 2021. The review of this article was arranged by Editor C.-M. Zetterling.

Digital Object Identifier 10.1109/JEDS.2020.3042264

1.3 kV Reverse-Blocking AlGaN/GaN MISHEMT With Ultralow Turn-On Voltage 0.25 V

HAIYONG WANG, WEI MAO, SHENGLEI ZHAO (Member, IEEE), MING DU, YACHAO ZHANG, XUEFENG ZHENG, CHONG WANG (Associate Member, IEEE), CHUNFU ZHANG (Member, IEEE), JINCHENG ZHANG (Member, IEEE), AND YUE HAO (Senior Member, IEEE)

Key Laboratory of Ministry of Education for Wide Band-Gap Semiconductor Materials and Devices, School of Microelectronics, Xidian University, Xi'an 710071, China

CORRESPONDING AUTHORS: W. MAO AND S. ZHAO (e-mail: wmao@xidian.edu.cn; slzhao@xidian.edu.cn)

This work was supported in part by the Key Research and Development Program of Shaanxi under Program 2020ZDLGY03-05; in part by the National Natural Science Foundation of China under Grant 61574112; and in part by the Wuhu and Xidian University special fund for Industry-University-Research Cooperation under Project XWYCXY-012019002.

ABSTRACT A reverse-blocking AlGaN/GaN metal-insulator-semiconductor high electron mobility transistor (RB-MISHEMT) is proposed and fabricated. Compared with the conventional MISHEMT with ohmic drain, the proposed device features a hybrid Schottky-ohmic drain with a low work function Tungsten (W), based on which the state-of-the-art ultralow turn-on voltage (V_{on}) of 0.25 V could be realized without degradation in on-state characteristics. In addition, the fabricated RB-MISHEMT exhibits the excellent reverse blocking voltage of -1332 V (at $V_{GS} = 0$ V) and forward blocking voltage of 1315 V (at $V_{GS} = -15$ V) with a specific on-resistance ($R_{on,sp}$) of 3.5 mΩcm^2, leading in the highest power figure-of-merit (FOM) of $>$ 494 MW/cm^2. The good thermal stability could also be observed in fabricated RB-MISHEMT. The corresponding operation mechanism of RB-MISHEMT are also revealed by Silvaco ATLAS simulations. These results demonstrate the great potential in power electronics applications.

INDEX TERMS AlGaN/GaN, HEMT, reverse blocking, ultralow turn-on voltage, hybrid Schottky-ohmic drain with tungsten.

I. INTRODUCTION

GaN-based high electron mobility transistors (HEMTs) have emerged as a promising candidate for next generation high-efficiency power electronics owing to their favorable trade-off between on-resistance (R_{on}) and breakdown voltage (BV) as well as inherent high-temperature operating capability [1]–[4]. Great efforts had been made to improve the forward blocking performance and significant progress had been achieved [5]–[7]. For many power applications, such as Class-S switch-mode amplifiers [8], bidirectional switches as crucial devices of AC-AC matrix converters [9]–[11], have attracted much attention in the development of GaN-based power devices with excellent bidirectional blocking capability.

Usually, a single integrated bidirectional blocking device, instead of using a discrete transistor in series with a discrete Schottky barrier diode (SBD), could achieve high blocking voltages under both forward and reverse drain biases, which can obviously reduce the parasitic elements and further improve the power conversion efficiency. Nowadays, the reverse blocking capability of GaN-based power devices are realized by integrating a SBD at drain electrode [12]–[18]. It is vital to reduce the forward turn-on voltage (V_{on}) caused by SBD because the lower V_{on} is helpful to decrease the on-state power loss and thus to improve the overall power efficiency. Various approaches, including the fully AlGaN barrier recessed drain structure, hybrid Schottky-ohmic drain and hybrid tri-anode Schottky drain with nanoscale fins, have been studied [14]–[18], and the lowest V_{on} has been reduced to 0.4 V up to now.

In this work, a reverse-blocking AlGaN/GaN metal-insulator-semiconductor HEMT (RB-MISHEMT) is proposed for the purpose of both excellent bidirectional blocking ability and low V_{on}. A low work function W (4.6 eV) is used in the hybrid Schottky-ohmic drain for the first time, by which V_{on} could effectively reduce

This work is licensed under a Creative Commons Attribution-NonCommercial-NoDerivatives 4.0 License. For more information, see https://creativecommons.org/licenses/by-nc-nd/4.0/

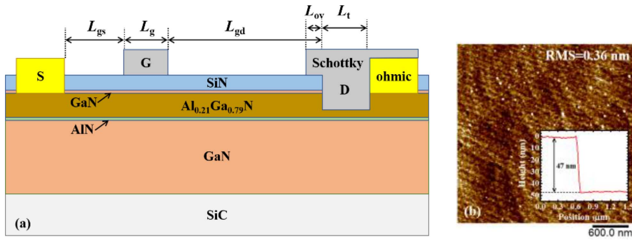

FIGURE 1. (a) Cross-sectional schematic of the RB-MISHEMT. (b) 3 μm × 3 μm surface morphology of recess drain area, inset: the height of the drain trench.

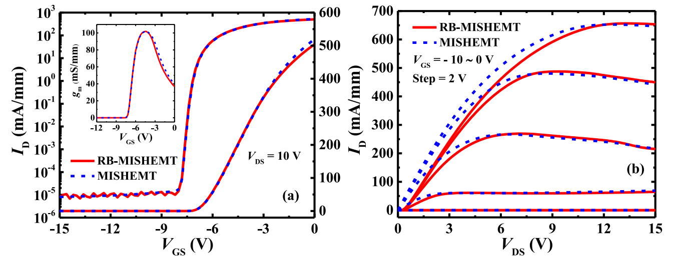

FIGURE 2. (a) Transfer and (b) output characteristics for RB-MISHEMT and MISHEMT with ohmic drain. The inset shows the transconductance performance for both devices.

to 0.25 V. A more than 1300 V bidirectional blocking voltage, the highest reverse figure-of-merit (FOM_R) of 509 MW/cm^2 and the highest forward figure-of-merit (FOM_F) of 494 MW/cm^2 could be achieved in the fabricated devices. Besides, the good thermal stability could be observed in RB-MISHEMT. Simulations with Silcavo have been conducted to further reveal the operation mechanism in RB-MISHEMT.

II. DEVICE STRUCTURE AND FABRICATION

A cross-sectional schematic of the proposed RB-MISHEMT is shown in Fig. 1(a). The device structure was grown on a 4-in semi-insulating SiC substrate by metal-organic chemical vapor deposition system (MOCVD). The epitaxial structure consists of a 2 nm undoped GaN cap layer, a 28 nm $Al_{0.21}Ga_{0.79}N$ barrier layer, a 1 nm AlN spacer layer, and a 1.6 μm undoped-GaN buffer layer. The Hall-effect measurement showed a sheet resistance of $\sim 377\Omega/\square$, a two-dimensional electron gas (2DEG) density of 7.9×10^{12} cm^{-2}, and an electron mobility of 2100 $cm^2/V \cdot s$.

The device fabrication started with 20 nm SiN passivation deposited by low pressure chemical vapor deposition (LPCVD). After removing the passivation layer in the source and drain area by RIE with CF_4/Ar, the ohmic metal Ti/Al/Ni/Au (= 22/140/55/45 nm) was directly deposited by E-beam evaporation, followed by rapid thermal annealing (RTA) at 850°C for 30 s in N_2 ambient to form the ohmic contact. Then a mesa isolation was realized by RIE etching. After SiN opening at the drain recess region, a low damage RIE etching process with an etch rate of 1.8 nm/min was performed to form the drain recess. A residual AlGaN barrier thickness of 3 nm is confirmed by AFM measurement as shown in Fig. 1(b), and the surface RMS roughness of the etched area is 0.36 nm. Next, the exposed AlGaN barrier surface was cleaned by a diluted HCl solution (HCl:H_2O = 1:20) followed by annealing at 450°C for 5 min in the N_2 ambient to recover the etch damage. Finally, the gate and drain Schottky metal W (200 nm) was simultaneously sputtered and patterned by lift-off, which was followed by an RTA process at 450°C for 5 min.

The conventional MISHEMT with ohmic drain (MISHEMT) has been also fabricated on the same wafer for reference. Unless otherwise specified, both devices have the same dimensions, in which gate-to-source distance (L_{gs}), gate length (L_g), gate-to-drain distance (L_{gd}), were 3 μm, 2 μm and 16 μm respectively. The L_{gd} for RB-MISHEMT refers to the distance between the gate and the drain recess region, and the drain recess width (L_t) and overlap extension (L_{ov}) were 5 μm and 1 μm, respectively. The gate width was 100 μm. Compared with the conventional HEMT, the proposed device features a recessed Schottky drain embedded into the ohmic drain electrode so as to lower V_{on}, blocking the reverse current flow to achieve reverse blocking.

III. RESULTS AND DISCUSSION

Fig. 2 shows the transfer and output characteristics of both devices. Nearly the same transfer curves could be observed in both devices with threshold voltage of −6.5 V, and maximum transconductance of 100 mS/mm and ON/OFF ratio of 10^7. A small differential on-resistance (r_{on}) and maximum I_D in RB-MISHEMT are 10.4 Ω·mm and 650 mA/mm, which are very close to the results in the referenced MISHEMT (R_{on} = 9.8 Ω·mm, I_D = 650 mA/mm). This demonstrates a slight influence of the recessed Schottky drain on the forward $I - V$ curves of RB-MISHEMT, compared with the counterpart. An ultralow V_{on} of 0.25 V (extracted at I_D = 1 mA/mm), a forward voltage (V_F) of 1.4 V (defined at 100 mA/mm), and an on-resistance of 14.6 Ω·mm (R_{on}, calculated at I_D = 100 mA/mm) are achieved in RB-MISHEMT. Here, the V_F at higher current drives (100 mA/mm) is considered, which is used to evaluate the device performance in the real applications. The ultralow V_{on} could be attributed to the obviously reduced Schottky barrier height realized by the partially recessed AlGaN barrier combined with a low work function W.

Log scale $I_D - V_{DS}$ curves of RB-MISHEMT at V_{GS} = 0 V are shown in Fig. 3(a), which presents rectification behavior for the hybrid Schottky-ohmic drain diode. And the extracted Schottky barrier height and ideality factor are 0.44 eV and 1.67, respectively. Fig. 3(b) shows the forward and reverse breakdown characteristics of RB-MISHEMT, and the forward breakdown characteristics of conventional MISHEMT. The forward breakdown voltage is 1272 V for conventional MISHEMT, while the forward breakdown voltage (BV_F) and reverse breakdown voltage (BV_R) are 1315 V and −1332 V at 10 μA/mm for RB-MISHEMT, respectively,

JOURNAL OF THE ELECTRON DEVICES SOCIETY

TABLE 1. Comparison of RB-MISHEMT in this work with reported reverse blocking GaN transistors in literatures.

	V_{on} (V) @ 1mA/mm	V_F (V) @ 100 mA/mm	$R_{on,sp}$ (mΩ·cm^2)	I_R (A/mm) @ V_{DS}=-100 V	BV_R (V)	FOM$_R$ (MW/cm^2)	BV_F (V)	FOM$_F$ (MW/cm^2)
[14]	~1.0	2.4	-	~10^{-2}	-110	-	-	-
[12]	1.7	2.8	0.49	-	-49	4.9	149	45
[15]	0.55	2.1	1.97	~2×10^{-5}	-321	52	351	63
[10]	1.5	3.6	3.1	-	-650	136	650	136
[16]	0.4	1.5	1.9	6×10^{-6}	-685	247	615	199
[17]	0.5	1.9	-	2×10^{-8}	-656	-	790	-
[18]	0.58	2.1	2.7	1.9×10^{-8}	-900	301	800	238
[13]	1.0	4.3	39.1	4×10^{-10}	< -3000	> 230	> 3000	> 230
This work	0.25	1.4	3.5	2×10^{-6}	-1332	509	1315	494

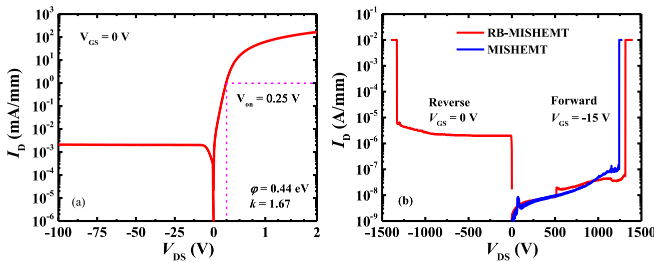

FIGURE 3. (a) Log scale $I_D - V_{DS}$ curves of RB-MISHEMT at $V_{GS} = 0$ V. (b) Forward and reverse breakdown characteristics of the RB-MISHEMT and MISHEMT.

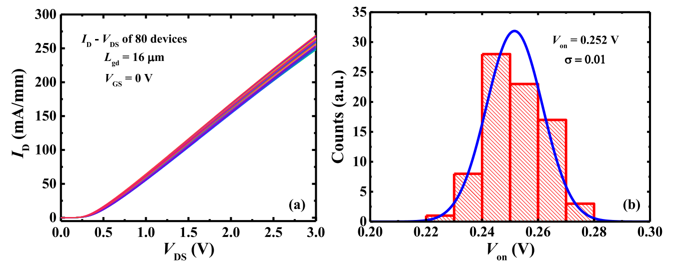

FIGURE 5. (a) Linear region at $V_{GS} = 0$ V of $I_D - V_{DS}$ output curves for 80 devices on the same wafer and (b) distribution of the extracted V_{on} at $I_D = 1$ mA/mm.

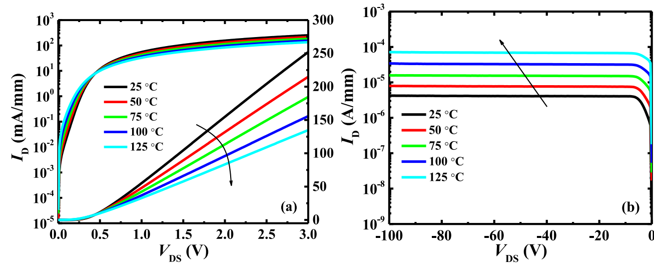

FIGURE 4. Forward (a) and reverse (b) $I_D - V_{DS}$ depended on the temperature in RB-MISHEMT.

which demonstrates great bidirectional blocking performance of RB-MISHEMT. The embedded hybrid Schottky-ohmic drain has little effect on the BV_F of RB-MISHEMT and achieves a high BV_R.

It is necessary to investigate the device behavior at high temperature because the actual temperature of GaN power devices could exceed 100°C during circuit operation [4]. The forward and reverse $I_D - V_{DS}$ characteristics of RB-MISHEMT depended on the temperature are plotted in Fig. 4. The V_{on} decreases from 0.25 V to 0.19 V and the R_{on} increases from 10.4 Ω·mm to 19.4 Ω·mm, with the temperature increasing from 25°C to 125°C. The increase of reverse leakage current at high temperature is due to the lower Schottky barrier and stronger thermionic emission at a reverse biased Schottky junction.

$I_D - V_{DS}$ curves for 80 devices are plotted in Fig. 5(a), demonstrating a high uniformity of the recessed hybrid Schottky-ohmic drain. Fig. 5(b) shows the distribution of the V_{on} for 80 devices extracted from Fig. 5(a) using 1 mA/mm as the criteria. The mean value of V_{on} is 0.252 V with a small standard derivation of 0.01 V.

The comparison of the proposed RB-MISHEMT with reported reverse blocking GaN devices is carried out in Table 1. Considering a 1.5 μm transfer length for each ohmic contact, the specific R_{on} ($R_{on,sp}$) for RB-MISHEMT is 3.5 mΩ·cm^2. By using the hybrid Schottky-ohmic drain and low work function W, the proposed RB-MISHEMT exhibits the lowest V_{on} of 0.25 V, the lowest V_F of 1.4 V, the highest FOM$_R$ of 509 MW/cm^2, and the highest FOM$_F$ of 494 MW/cm^2. And the trade-off between BV and $R_{on,sp}$ is shown in Fig. 6. A good trade-off between BV and $R_{on,sp}$ is achieved of the fabricated RB-MISHEMT among the reported reverse blocking devices. In addition, there is a trade-off between the V_{on} and the reverse leakage current, which is attributed to a lower V_{on} (namely representing a lower barrier height) leading to a large reverse leakage current. Fig. 7 shows the V_{on} versus reverse leakage current benchmark of RB-MISHEMT against the reported GaN low V_{on} rectifiers. As shown, the RB-MISHEMT also shows a relatively good trade-off between V_{on} and reverse leakage current among the reported counterparts.

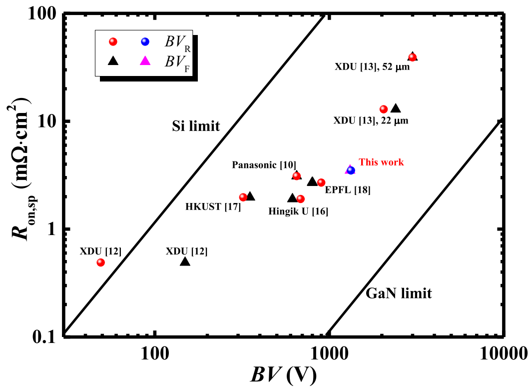

FIGURE 6. BV_F and BV_R versus $R_{on,sp}$ benchmark of reverse-blocking GaN HEMTs.

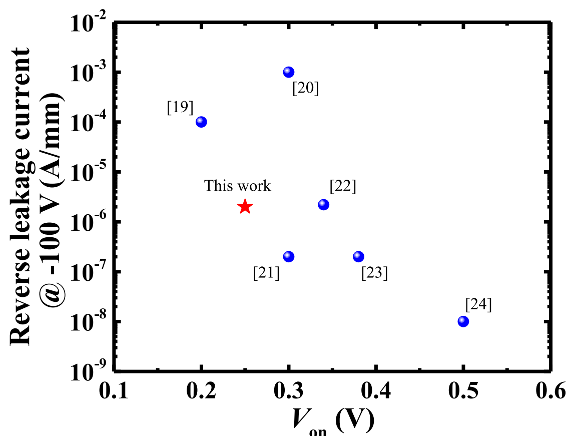

FIGURE 7. Comparison of V_{on} and reverse leakage current @ -100 V with reported GaN low V_{on} rectifiers.

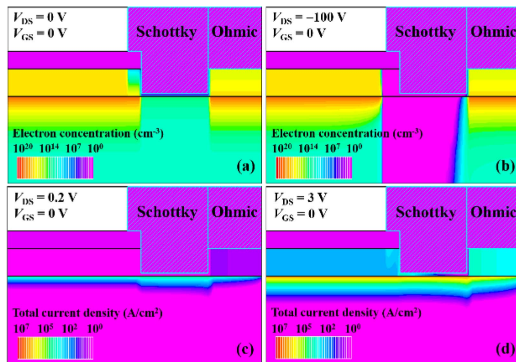

FIGURE 8. Simulated electron concentration distribution at the Schottky-ohmic drain region with (a) $V_{DS} = 0$ V and (b) $V_{DS} = -100$ V and total current density distribution with (c) $V_{DS} = 0.2$ V and (d) $V_{DS} = 3$ V.

These results demonstrate the great potential of the proposed RB-MISHEMT as unidirectional power transistors.

In order to further investigate the operation mechanism of RB-MISHEMT, the proposed device is simulated by Silvaco ATLAS. The RB-MISHEMT operation mechanism is illustrated in Fig. 8(a)–(d). As shown in Fig. 8(a), the Schottky

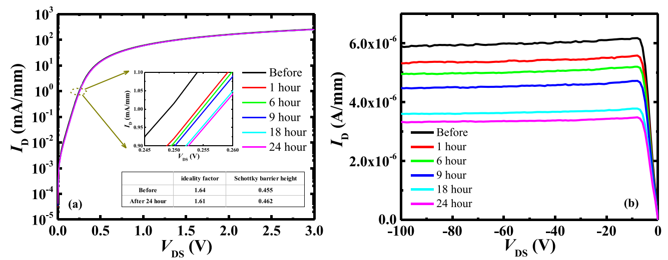

FIGURE 9. The variation of forward and reverse $I_D - V_{DS}$ characteristics of RB-MISHEMT after thermal storage at 200°C for different time.

metal of hybrid drain in the recess region is used to completely deplete the 2DEG under the recessed AlGaN at $V_D = 0$ V. The depletion function is similar to the gate depletion in the recessed normally-off GaN HEMT. When the drain electrode is biased at negative voltage $V_D = -100$ V in Fig. 8(b), the depletion region near the drain will be further expanded by the reverse biased Schottky junction. The overlap extension (L_{ov}) could work as a field plate (FP) to relieve the high electric field near recessed Schottky junction. On the other hand, when the drain bias is increased from 0 V to a small positive voltage 0.2 V in Fig. 8(c), the channel under the recessed Schottky will not be depleted, and a small drain current begins to flow from ohmic drain to the source. With the increase of drain voltage, the hybrid Schottky drain is turned on, and the drain current is composed of Schottky drain current and ohmic drain current [22], leading to ultralow turn-on voltage of 0.25 V. When a relatively large voltage 3 V is applied to the drain electrode in Fig. 8(d), the conduction current is very large and comparable to conventional MISHEMT. The depth of recess drain is very important for the ultralow V_{on} of RB-MISHEMT. And there is a trade-off between V_{on} and the reverse leakage current. If the residual AlGaN barrier is too thick, the 2DEG under the recess will not be depleted by the Schottky drain, which is similar to the ohmic drain and thus leads to a serious reverse leakage current. When the recess depth is larger than the thickness of AlGaN barrier, the ohmic drain will play no role in the forward current conduction.

The thermal stability and long-term reliability of this device have been considered. Thermal storage tests are carried out at 200°C for different time to evaluate the influence of Schottky-ohmic drain stability on the device performance. As shown in Fig. 9. the forward and reverse $I_D - V_{DS}$ characteristics of Schottky-ohmic drain before and after thermal storage testing at 200°C are compared. An increase in Schottky barrier height and a decrease in ideality factor after thermal storage at 200°C for 24 hours could be observed. In addition, the reverse leakage current is reduced as the increase in time. These results are attributed to the reduction of interfacial layer at the W Schottky interface after thermal storage, leading to a more ideal diode with a higher Schottky barrier height. Besides, the rearrangement of the

interface material structure might prevent the excess leakage current [25], [26]. These demonstrate the good thermal stability of RB-MISHEMT.

IV. CONCLUSION

In this work, we have experimentally demonstrated the high-performance RB-MISHEMT based on hybrid Schottky-ohmic drain and low work function W techniques. The proposed device exhibits an ultralow V_{on} of 0.25 V, a high forward BV_{F} of 1315 V and a reverse BV_{R} of −1332 V. Compared with current reported reverse blocking GaN HEMTs, a better trade-off between BV and $R_{\text{on,sp}}$ has been achieved. Besides, the good thermal stability could be observed in RB-MISHEMT. Simulations are performed for the clear explanation of the operation mechanism of RB-MISHEMT. These results demonstrate the excellent performance of reverse blocking devices.

REFERENCES

[1] Y.-F. Wu, J. Gritters, L. Shen, R. P. Smith, and B. Swenson, "kV-class GaN-on-Si HEMTs enabling 99% efficiency converter at 800 V and 100 kHz," *IEEE Trans. Power Electron.*, vol. 29, no. 6, pp. 2634–2637, Jun. 2014, doi: 10.1109/TPEL.2013.2284248.

[2] Y. Wu, M. Jacob-Mitos, M. L. Moore, and S. Heikman, "A 97.8% efficient GaN HEMT boost converter with 300-W output power at 1 MHz," *IEEE Electron Device Lett.*, vol. 29, no. 8, pp. 824–826, Aug. 2008, doi: 10.1109/LED.2008.2000921.

[3] T. Oka and T. Nozawa, "AlGaN/GaN recessed MIS-gate HFET with high-threshold-voltage normally-off operation for power electronics applications," *IEEE Electron Device Lett.*, vol. 29, no. 7, pp. 668–670, Jul. 2008, doi: 10.1109/LED.2008.2000607.

[4] K. J. Chen *et al.*, "GaN-on-Si power technology: Devices and applications," *IEEE Trans. Electron Devices*, vol. 64, no. 3, pp. 779–795, Mar. 2017, doi: 10.1109/TED.2017.2657579.

[5] W. Saito *et al.*, "Field-plate structure dependence of current collapse phenomena in high-voltage GaN-HEMTs," *IEEE Electron Device Lett.*, vol. 31, no. 7, pp. 659–661, Jul. 2010, doi: 10.1109/LED.2010.2048741.

[6] M. Zhu, J. Ma, L. Nela, C. Erine, and E. Matioli, "High-voltage normally-off recessed tri-gate GaN power MOSFETs with low on-resistance," *IEEE Electron Device Lett.*, vol. 40, no. 8, pp. 1289–1292, Aug. 2019, doi: 10.1109/LED.2019.2922204.

[7] H. Wang, F. J. Lumbantoruan, T. Hsieh, C. Wu, Y. Lin, and E. Y. Chang, "High-performance LPCVD-SiN_x/InAlGaN/GaN MIS-HEMTs with 850 V 0.98m·cmΩ^2 for power device applications," *IEEE J. Electron Devices Soc.*, vol. 6, pp. 1136–1141, 2018, doi: 10.1109/JEDS.2018.2869776.

[8] R. Leberer, R. Reber, and M. Oppermann, "An AlGaN/GaN class-S amplifier for RF-communication signals," in *Proc. Int. Microw. Symp.*, Atlanta, GA, USA, Jun. 2008, pp. 85–88, doi: 10.1109/MWSYM.2008.4633109.

[9] P. W. Wheeler, J. Rodriguez, J. C. Clare, L. Empringham, and A. Weinstein, "Matrix converters: A technology review," *IEEE Trans. Ind. Electron.*, vol. 49, no. 2, pp. 276–288, Apr. 2002, doi: 10.1109/41.993260.

[10] T. Morita *et al.*, "650 V 3.1 mΩ·cm^2 GaN-based monolithic bidirectional switch using normally-off gate injection transistor," in *IEEE Int. Electron Devices Meeting (IEDM) Tech. Dig.*, Washington, DC, USA, Dec. 2008, pp. 865–868, doi: 10.1109/IEDM.2007.4419086.

[11] E. R. Motto, J. F. Donlon, M. Tabata, H. Takahashi, Y. Yu, and G. Majumdar, "Application characteristics of an experimental RB-IGBT (reverse blocking IGBT) module," in *Proc. IEEE Ind. Appl. Conf. 39th IAS Annu. Meeting Conf. Rec.*, vol. 3. Seattle, WA, USA, Oct. 2004, pp. 1540–1544, doi: 10.1109/IAS.2004.1348675.

[12] S. L. Zhao *et al.*, "Mechanism of improving forward and reverse blocking voltages in AlGaN/GaN HEMTs by using Schottky drain," *Chin. Phys. B*, vol. 23, no. 10, Oct. 2014, Art. no. 107303, doi: 10.1088/1674-1056/23/10/107303.

[13] Y. H. Wu *et al.*, "More than 3000 V reverse blocking schottky-drain AlGaN-channel HEMTs with > 230 MW/cm^2 power figure-of-merit," *IEEE Electron Device Lett.*, vol. 40, no. 11, pp. 1724–1727, Nov. 2019, doi: 10.1109/LED.2019.2941530.

[14] E. Bahat-Treidel, R. Lossy, J. Wurfl, and G. Trankle, "AlGaN/GaN HEMT with integrated recessed Schottky-drain protection diode," *IEEE Electron Device Lett.*, vol. 30, no. 9, pp. 901–903, Sep. 2009, doi: 10.1109/LED.2009.2026437.

[15] C. Zhou, W. Chen, E. L. Piner, and K. J. Chen, "Schottky-ohmic drain AlGaN/GaN normally off HEMT with reverse drain blocking capability," *IEEE Electron Device Lett.*, vol. 31, no. 7, pp. 668–670, Jul. 2010, doi: 10.1109/LED.2010.2048885.

[16] J.-G. Lee, S.-W. Han, B.-R. Park, and H.-Y. Cha, "Unidirectional AlGaN/GaN-on-Si HFETs with reverse blocking drain," *Appl. Phys. Exp.*, vol. 7, no. 1, Dec. 2013, Art. no. 014101, doi: 10.7567/APEX.7.014101.

[17] J. C. Lei *et al.*, "Reverse-blocking normally-OFF GaN double-channel MOS-HEMT with low reverse leakage current and low on-state resistance," *IEEE Electron Device Lett.*, vol. 39, no. 7, pp. 1003–1006, Jul. 2018, doi: 10.1109/LED.2018.2832180.

[18] J. Ma, M. Zhu, and E. Matioli, "900 V reverse-blocking GaN-on-Si MOSHEMTs with a hybrid tri-anode Schottky drain," *IEEE Electron Device Lett.*, vol. 38, no. 12, pp. 1704–1707, Dec. 2017, doi: 10.1109/LED.2017.2761911.

[19] M. Basler *et al.*, "Large-area lateral AlGaN/GaN-on-Si field-effect rectifier with low turn-on voltage," *IEEE Electron Device Lett.*, vol. 41, no. 7, pp. 993–996, Jul. 2020, doi: 10.1109/LED.2020.2994656.

[20] W. Chen, W. Huang, K. Y. Wong, and K. J. Chen, "High-performance AlGaN/GaN HEMT-compatible lateral field-effect rectifiers," in *Proc. Device Res. Conf.*, Santa Barbara, CA, USA, Jun. 2008, pp. 287–288, doi: 10.1109/DRC.2008.4800842.

[21] Q. Zhou *et al.*, "Lateral AlGaN/GaN power diode with MIS-gated hybrid anode for ultra-low turn-on voltage and high breakdown voltage," in *Proc. 14th China Int. Forum Solid State Light. Int. Forum Wide Bandgap Semicond. China (SSLChina: IFWS)*, Nov. 2017, pp. 168–171, doi: 10.1109/IFWS.2017.8246001.

[22] J. Lee, B. Park, C. Cho, K. Seo, and H. Cha, "Low turn-on voltage AlGaN/GaN-on-Si rectifier with gated ohmic anode," *IEEE Electron Device Lett.*, vol. 34, no. 2, pp. 214–216, Feb. 2013, doi: 10.1109/LED.2012.2235403.

[23] T. Zhang *et al.*, "A > 3 kV/2.94 m?·cm^2 and low leakage current with low turn-on voltage lateral GaN Schottky barrier diode on silicon substrate with anode engineering technique," *IEEE Electron Device Lett.*, vol. 40, no. 10, pp. 1583–1586, Oct. 2019, doi: 10.1109/LED.2019.2933314.

[24] J. Hu *et al.*, "Performance optimization of au-free lateral AlGaN/GaN Schottky barrier diode with gated edge termination on 200-mm silicon substrate," *IEEE Trans. Electron Devices*, vol. 63, no. 3, pp. 997–1004, Mar. 2016, doi: 10.1109/TED.2016.2515566.

[25] M. Zhao, X. H. Wang, X. Y. Liu, J. Huang, Y. K. Zheng, and K. Wei, "Thermal storage of AlGaN/GaN high-electron-mobility transistors," *IEEE Trans. Device Mater. Rel.*, vol. 10, no. 3, pp. 360–365, Sep. 2010, doi: 10.1109/TDMR.2010.2051671.

[26] S. Singhal *et al.*, "GaN-on-Si failure mechanisms and reliability improvements," in *Proc. IEEE 44th Annu. Int. Rel. Phys. Symp.*, San Jose, CA, USA, Mar. 2006, pp. 95–98, doi: 10.1109/RELPHY.2006.251197.